

Hydrophilic Interactions between Organic and Water Molecules as Models for Monolayers at the Gas/Water Interface

A. Ivanova,* A. Tadjer, N. Tyutyulkov, and B. Radoev

University of Sofia, Faculty of Chemistry, Chair of Physical Chemistry, 1 James Bourchier Ave., 1164 Sofia, Bulgaria

Received: November 24, 2004

Model clusters of surfactant prototypes with small number of water molecules are calculated at different levels of theory. All approaches used yield correct trends in the variation of the dipole moment upon tail elongation or polar headgroup variation. Models including one, two, or more water molecules are optimized. The most stable structures are those with maximum number of atoms involved in hydrogen bonding. The normal components of the dipole moment prove to be less sensitive to the nature (aliphatic or aromatic) of the hydrophobic tail, in accord with findings from the phenomenological models. Values of the dipole moment approaching the experimental estimates required inclusion of sufficient aqueous environment (>20 water molecules per hydrophilic head) and of lateral intersurfactant interactions into the model.

Introduction

Insoluble monolayers have been subject to scientific investigation for almost a decade. A substantial amount of experimental data concerning structure, rheology and various physicochemical characteristics of different monolayers is accumulated. The interest toward insoluble surfactant monolayers at the air/water interface stems from the fact that they are suitable models of biological membranes or of heterogeneous interfaces in general.¹

Insoluble monolayers formed at the water surface are studied by means of a number of specific techniques.^{2–5} The oldest and the most routine one used for rheological experiments is the measurement of surface pressure (surface potential) by means of film compression in a Langmuir trough. The measured surface potential (ΔV) is usually related to the effective dipole moment of the monolayer in a direction normal to the water surface, μ_{\perp} .¹ There are several phenomenological models for interpretation of surface potential data.^{1,6–8} However, all of them provide approximate values of the normal dipole moment, since some of the employed parameters are either experimentally inaccessible (dielectric constant of the monolayer, ϵ) or estimated in an approximate manner (group dipole moments are assumed to be summed bond dipole moments). Another disadvantage of the models is that they usually assume the rearrangement of the water molecules around the hydrophilic surfactant headgroups insignificant or the structure of the water in the vicinity of different headgroups identical.

All these drawbacks are due to the lack of information about the microscopic characteristics of the film-forming molecules and their environment, e.g., the arrangement of the closest water molecules. Some of the shortcomings can be avoided with the help of theoretical (quantum chemical) simulations of insoluble monolayers. Such molecular models allow optimization of the structure, the organization and the molecular characteristics of amphiphilic molecules at the gas/water interface. Moreover, a correct quantum chemical simulation includes all types of

essential interactions within the monolayer—van der Waals, electrostatic, hydrogen bonding, etc., without artificial partitioning of the system into separate noninteracting fragments (as done in most of the phenomenological models^{6–8}). Another advantage is the possibility of estimation of the normal and tangential components of various parameters of interest; i.e., account is taken of the anisotropy at the interface.

So far, there are a number of communications dealing with theoretical simulation of insoluble monolayers at the water surface.^{9–13} The majority are based on molecular mechanics and/or Monte Carlo conformational analysis. The interface layer is modeled either as an abrupt boundary between two continua with substantial difference in dielectric constants^{12,13} or with linear gradient of ϵ in the monolayer region.¹⁰ The rest of the papers report quantum chemical calculations of the surfactant molecules in vacuo.^{9,11} The solvent water molecules are not treated explicitly in any of these studies. However, the specific intermolecular interactions between the hydrophilic surfactant head and the closest surrounding water molecules may be the critical factor determining the overall behavior of the monolayer, since the neighboring water molecules contribute substantially to the microenvironment of the surfactant headgroups, i.e., the local dielectric medium, the orientation of the polar groups, etc.

Quantum chemical semiempirical or ab initio modeling of the hydrophilic interactions between polar surfactant headgroups and the closest-contact water molecules would provide information about the active role of water as a monolayer counterpart, not just as a solvent medium. The purpose of this paper is to present and discuss the results from a set of quantum chemical models describing explicitly the interaction between different surfactant prototypes and various number of water molecules.

Surfactant Prototypes

The first step in the investigation is a comparison of the accuracy of different computational methods in reproducing the structure and the dipole moments, μ , of a series of organic molecules used in subsequent monolayer models. The molecules studied are shown in Figure 1.

* Corresponding author. Fax +3592-962-54-38. E-mail: fhai@chem.uni-sofia.bg.

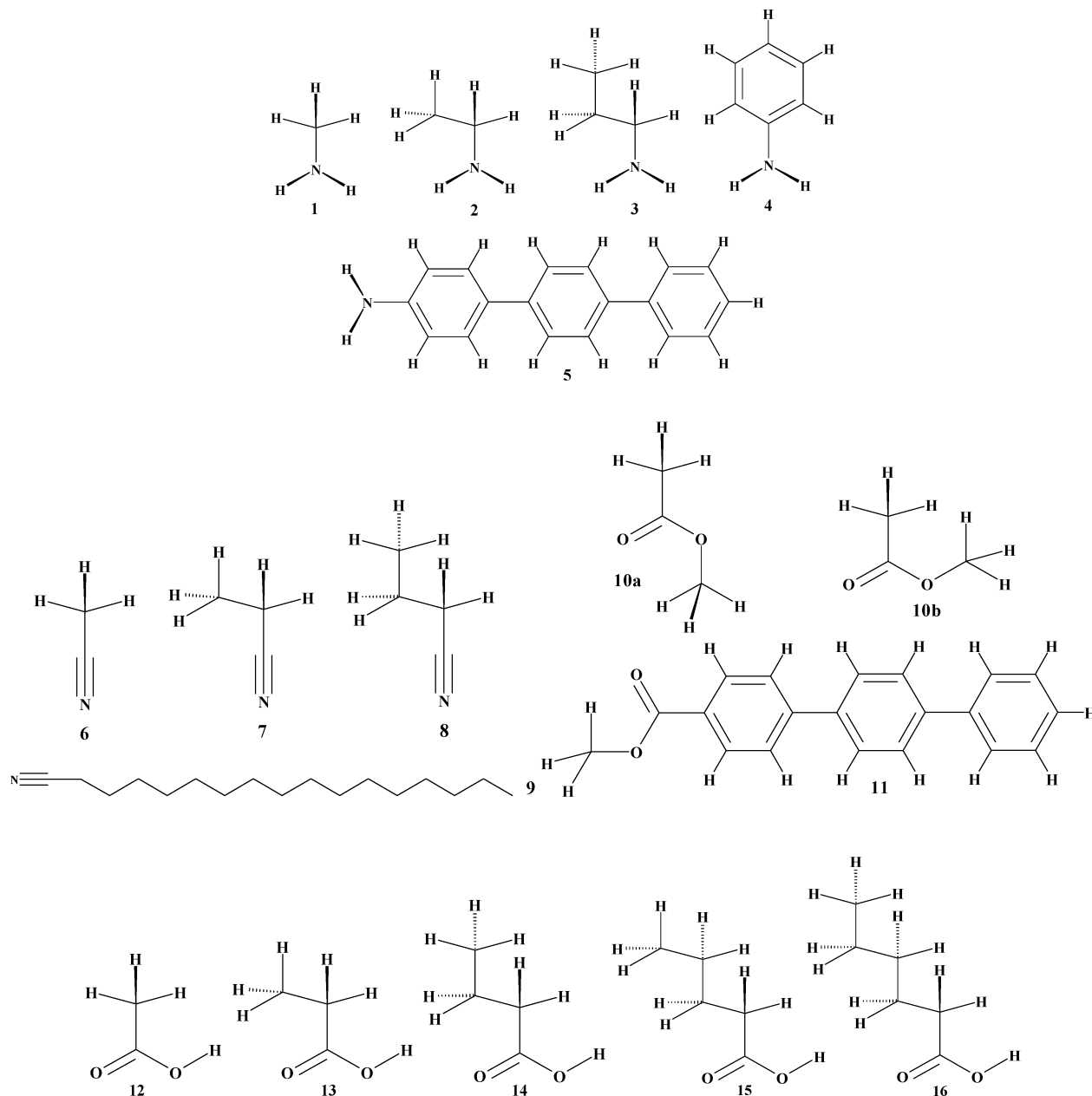


Figure 1. Chemical formulas of the studied organic molecules: **1**, methylamine; **2**, ethylamine; **3**, propylamine; **4**, aniline; **5**, 4-amino-*p*-terphenyl; **6**, methyl nitrile; **7**, ethyl nitrile; **8**, propyl nitrile; **9**, octadecyl nitrile; **10**, methyl acetate; **11**, 4-carbomethoxy-*p*-terphenyl; **12**, ethanoic (acetic) acid; **13**, propanoic acid; **14**, butanoic acid; **15**, pentanoic acid; **16**, hexanoic acid.

Monolayers of three of the selected molecules (**5**, **9**, **11**) have been characterized experimentally by Demchak and Fort during the development of their three-capacitor model.⁶ Thus, it is interesting to check whether the calculated dipole moments will match the values obtained by means of the three-capacitor approach. The major part of the chosen molecules (**1–4**, **6–8**, **10**) consists of short-tail analogues of the surfactants investigated by Demchak and Fort. They contain one polar functional group bound to a hydrophobic hydrocarbon tail of varying length and nature. Furthermore, there are experimental values for the dipole moments of all molecules represented in Figure 1. This allows verification both of the reproducibility of the experimental dipole moments and of the correct tendency in the variation of μ upon elongation of the hydrophobic tail. Finally, a set of aliphatic carboxylic acids is included (**12–16**), since the insoluble monolayers of the long-chain analogues are among the most intensively investigated in the field.^{14–16}

Further on, some of the molecules are used for construction of monolayer models involving different number of water molecules (see below).

Computational Details

Geometry optimization of the isolated molecules is performed with a variety of methods. Within the molecular mechanics framework, the MM+ force field is used.¹⁷ The electrostatic potential is modeled in monopole approximation (atomic charges). The atomic charges are adopted from an AM1 calculation of the isolated molecules in vacuo. At semiempirical level all geometry optimizations and dipole moments determination are done with AM1.¹⁸ The ab initio calculations are with the RHF method, standard STO-3G or 6-31G basis sets, as included in GAUSSIAN W03.¹⁹ The semiempirical and molecular mechanics methods employed are as implemented in the HYPERCHEM 7.03 program package.²⁰

TABLE 1: Dipole Moment (in D) for the Optimized Structures in Vacuo of Molecules 1–16 (Figure 1) Calculated with Different Methods^a

molecule	MM+	AM1	STO-3G	6-31G	experiment ^{6,21}
1	0.118	1.493	1.617	1.254	1.28 (g), 1.46 (B)
2	0.107	1.466	1.556	1.216	1.22 (g), 1.38 (B)
3	0.081	1.416	1.530	1.261	1.17 (g)
4	0.299	1.583	1.327	1.454	1.53
5	0.377	2.384	1.930	2.277	−0.095 (a/w)
6	0.237	2.894	3.097	4.135	3.97
7	0.195	2.938	3.205	4.245	4.02 (g), 3.56 (B)
8	0.504	3.001	3.284	4.363	4.07
9	0.554	3.105	3.403	4.605	0.575 (a/w)
10a	0.403	1.754	0.880	2.024	1.75 (B)
10b	0.817	4.500	3.287	5.681	
11	0.513	2.605	1.292	2.661	0.380 (a/w)
12	0.422	1.891	0.796	1.880	1.74 (g)
13	0.451	1.843	0.897	2.032	1.75 (g)
14	0.548	1.863	0.942	2.127	1.90 (B)
15	0.561	1.853	0.959	2.155	1.90 (B)
16	0.565	1.865	0.977	2.203	1.90 (g)

^a The experimental values for the isolated molecules are taken from ref 21 and those at the air/water interface from ref 6. Key: (g) the measurement is from the gas phase; (B) the measurement is in benzene solution; (a/w) normal component of the monolayer dipole moment at the air/water interface, estimated with the three-capacitor model.

The clusters containing one organic and one or two water molecules are optimized either with AM1 or with RHF/6-31G. For the clusters containing more organic and/or water molecules, solely AM1 is used.

Results and Discussion

1. Isolated Molecules. The structures of all molecules in Figure 1 are optimized with MM+, AM1, RHF/STO-3G, or RHF/6-31G. The total dipole moments, as well as the *x*, *y*, and *z* components, of the optimized molecules are calculated with the corresponding method used for the geometry optimization. The results are shown in Table 1.

In all cases the tendency in the variation of the dipole moment upon tail elongation is correct. Comparison of the obtained dipole moments of the small molecules with the experimental data reveals, as expected, that the gas-phase measurements are reproduced best by the ab initio method with larger basis set. The mean deviation for the series **1–4**, **6–8**, and **10** is $\approx 6\%$. The experimental values for the series of carboxylic acids **12–16** are not reproduced so well, the mean deviation being $\sim 13\%$, but the agreement is still fair. However, the constant value of the dipole moment upon tail elongation is achieved promptly. The latter is valid also for the dipole moments calculated with the semiempirical AM1 method. The AM1 values match more closely the ones measured in the nonpolar solvent (for the amines and the methyl acetate the agreement is quantitative). This is due to the parametrization of the AM1 method. Apparently, the dipole moments produced by the molecular mechanics force field are highly underestimated. This discrepancy arises from the way the MM+ electrostatic term is modeled, i.e., from the monopole approximation. On the other hand, the MM+ dipole moments are closer to those estimated from monolayer surface potential measurements. This is to be expected, since the phenomenological model treats the monolayer as constructed from point dipoles.

In summary, the above results indicate that RHF/6-31G, AM1, and MM+ are prospective methods for estimation of the electrical properties of molecules forming monolayers at the air/water interface provided that some additional factors are accounted for, while the ab initio approach with small basis set

RHF/STO-3G fails to reproduce even the dipole moments of the isolated molecules in vacuo. Another outcome is that such monolayer properties as the dipole moment cannot be simulated solely by calculations on the surfactant molecules in vacuo. The values of the computed total dipole moments of the isolated molecules, as well as their “normal” components (if it is assumed that the axis connecting the heteroatom from the functional group with the first carbon from the tail is normal to the film, i.e., that the molecules are perpendicular to an imaginary water surface), differ substantially from the numbers yielded by all phenomenological models for interpretation of the measured surface potential. In our opinion, the mismatch is due mainly to the neglect of the aqueous environment around the hydrophilic heads in all above-mentioned calculations.

Therefore, several models, including part of the adjacent water molecules, are suggested further.

2. Clusters Involving a Small Number of Water Molecules. First, one water molecule is added to **1** and **6** (cf. Figure 1) (the amine and the nitrile serving as models of hydrophilic heads of different nature), and the structure of the cluster is optimized at the RHF/6-31G level. Three starting orientations of the water molecule around the amino group of methylamine are studied, while for acetonitrile we consider the most probable arrangement of the two molecules as unequivocally defined. The latter is asymmetric because we avoid intentionally any symmetric restrictions. All starting geometries are shown in Figure 2.

The three structures of **1** relax to the same minimum energy structure, represented in Figure 3 together with its dipole moment. The data for the optimized geometry of the cluster of **6** are shown in Figure 3 as well.

The normal dipole moments are calculated on the assumption that the film normal coincides with the C–N bond. Both clusters feature substantial increase of the total and of the normal dipole moment (μ_{\perp} increases by more than 2 D) compared to μ of the organic molecules in vacuo. This arises from the increased distance between the centers of the positive and the negative charges. While the center of the positive charges remains in the hydrocarbon fragments, the negative end of the dipole has been displaced somewhere between the nitrogen and the oxygen atoms. Moreover, the increase in the charge separation is essentially in the normal direction.

Both for **1** and **6** the water molecule is oriented with one of its hydrogen atoms pointing toward the nitrogen atom of the amine/nitrile group. The N–H distance is typical for a hydrogen bond, the latter being stronger in the amine cluster (ammonia-type structure).

The next step in the modeling of the aqueous environment represents the introduction of a second water molecule. This brings about a large number of possible mutual arrangements of the three molecules in the cluster. However, just a few of them, featuring significantly different orientations of the three molecules, are studied. Clusters of **1**, **4** and **5**, each with two water molecules, are constructed. First, three different amines are chosen in order to follow the influence of the nature of the hydrophobic tail on the water molecules orientation around an identical polar head.

The starting structures with different arrangement of the two water molecules around methylamine are presented in Figure 4:

In clusters **a** and **b** each oxygen from the water molecules is positioned near an amine hydrogen atom. The two models differ only in the direction of the water hydrogen atoms. In **a** they are in a plane perpendicular to the amino hydrogens, while in **b** all hydrogen atoms reside in one plane. Cluster **c** features

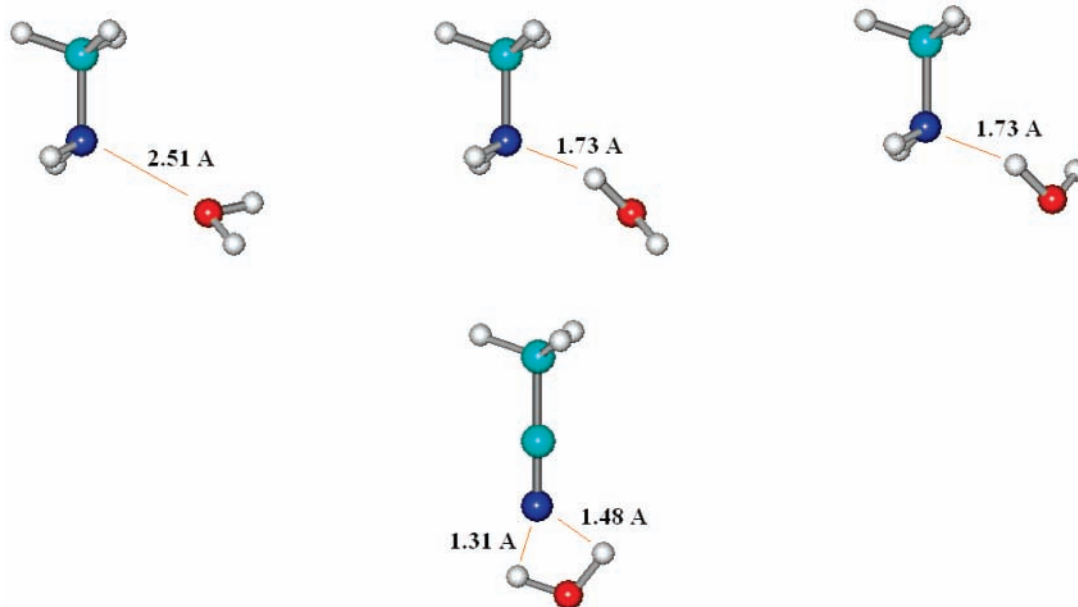


Figure 2. Starting orientation of one water molecule around the polar headgroup of methylamine (top) and methylnitrile (bottom).

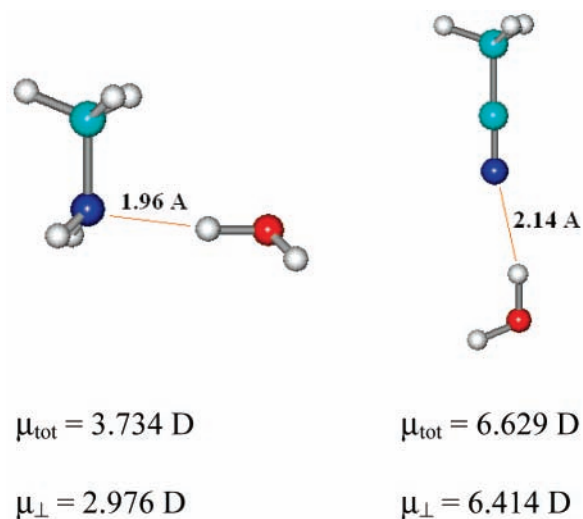


Figure 3. Dipole moments and H-bond length of RHF/6-31G optimized structures of methylamine (left) and methylnitrile (right) with one water molecule.

TABLE 2: RHF/6-31G Total Energy (E_{tot}) and Total (μ_{tot}) and “Normal” (μ_{\perp}) Dipole Moments of Methylamine Clusters with Two Water Molecules (cf. Figure 5 for Structure Notation)

structure	E_{tot} , kcal/mol	μ_{tot} , D	μ_{\perp} , D
a	-155104.8	1.584	1.070
b	-155094.3	4.785	0.497
c	-155101.6	1.268	0.374

coordination of the first water molecule to amino hydrogen and the second water molecule is coupled to the nitrogen.

The optimized structures are shown in Figure 5. Structures **a** and **c** look alike, and their energies are much lower than that of **b** (Table 2). The main difference between the two sets of structures is the number of hydrogen bonds formed—in arrangement **b**, the two water molecules form separate hydrogen bonds with the nitrogen and with one of the methylamine hydrogens, while the other two geometries feature an additional hydrogen bond between the two water molecules. This reveals a tendency for stabilization of structures with maximum number of both water–surfactant and water–water hydrogen bonds.

The calculated dipole moments corresponding to the three optimized methylamine clusters are shown in Table 2. The structures with low and high energy feature essentially different total dipole moments. For **a** and **c**, μ is much smaller due to the partial charge compensation from the additional hydrogen bond. The total dipole moments of the two low-energy geometries are slightly higher than μ of the isolated methylamine, which indicates that the dipole moments of the two water molecules cancel out each other almost completely. This is confirmed by the fact that **a** and **c** have smaller dipole moments than the cluster with one water molecule, while in **b** μ has grown by about 1 D relative to the value of the cluster with one water molecule. Despite the similar total dipole moments, the normal components of **a** and **c** differ considerably. The small μ_{\perp} in **c** is due to the fact that the dipole moment of one of the water molecules is virtually parallel to the normal but directed opposite to μ of methylamine. Comparison to experimental data may be indicative of the possible tilt angle in real monolayers, although the model is too rough to go further in these speculations.

On the basis of the above results, showing preference to structures with maximum number of hydrogen bonds, the starting alignment of the two molecules around aniline is chosen to have as many close contacts between hydrogens and heteroatoms as possible (Figure 6). AM1 and RHF/6-31G optimizations lead to the minimum energy structures and their corresponding dipole moments shown in Figure 7.

The main structural difference between the geometries yielded by the two methods is that according to AM1 the most stable structure involves strong hydrogen bonds between each water molecule and an amine hydrogen (the amine nitrogen is weakly coordinated to one of the water hydrogens, at distance 2.85 Å). On the other hand, the *ab initio* calculation gives preference to a “cyclic” type of structure, in which the amine nitrogen also participates in a strong hydrogen bond. This structure is similar to the minimum energy arrangement for methylamine with two water molecules, which means that *the type of the hydrocarbon residue* (aliphatic or aromatic) *does not alter* appreciably the orientation of the water molecules around the same hydrophilic head.

Regarding the electrical properties of the aniline cluster, the dipole moments calculated by the two methods differ too, as

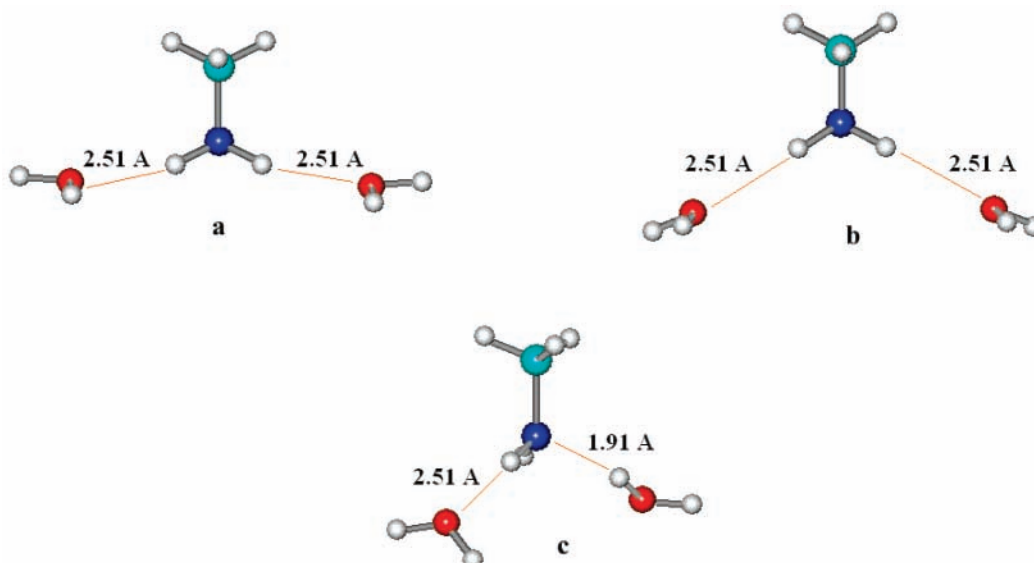


Figure 4. Scheme of the starting geometries of clusters built of methylamine and two water molecules.

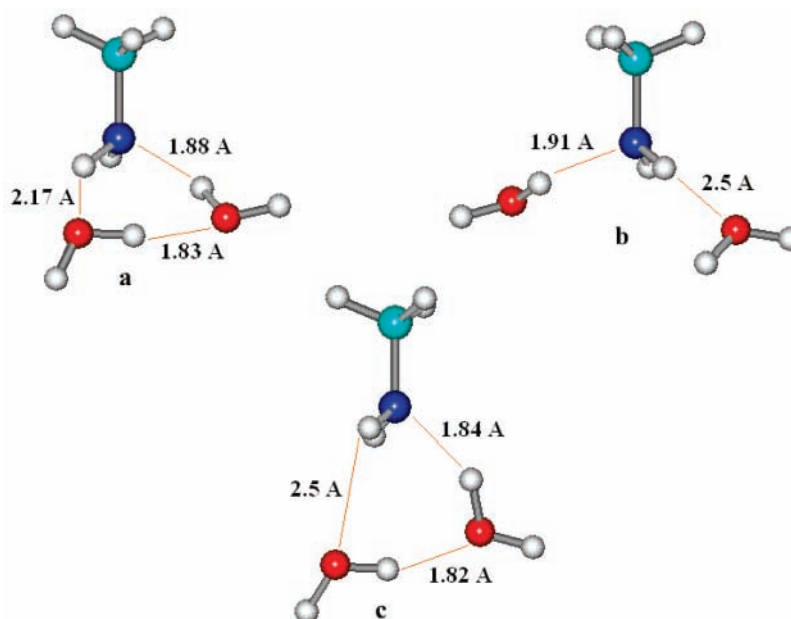


Figure 5. RHF/6-31G optimized structures of methylamine with two water molecules.

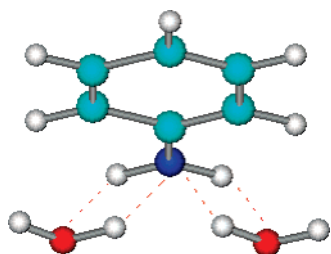


Figure 6. Scheme of the initial arrangement in a cluster containing one aniline and two water molecules.

implied by the structural dissimilarity. RHF/6-31G predicts substantial compensation of the water dipole moments, while with AM1 μ rises more than twice with respect to the isolated molecule. However, μ_{\perp} of the two clusters is of the same order of magnitude and similar to that of methylamine; i.e., it seems that μ_{\perp} is *less sensitive* to the change of the hydrocarbon substituents, in accordance with the results obtained phenomenologically by Dynarowicz-Latka et al.^{11c,22}

The starting structure from Figure 6 is used also for optimizing clusters of 4-amino-*p*-terphenyl with two water molecules. The results shown in Figure 8 are obtained. The AM1 and RHF/6-31G optimized structures are quite similar to the aniline ones—both the arrangement of the water molecules and the number of hydrogen bonds are preserved for each method.

Concerning the total dipole moments, the AM1 value is smaller than the one for aniline. This is due to the extended aromatic residue involved in effective conjugation with the benzene ring, which is directly bound to the amino group. The normal component of μ also decreases by 20% relative to the cluster of **4**, since the extension of the aromatic system is mostly along the normal.

The total and the normal dipole moments calculated with RHF/6-31G, however, increase by $\sim 30\%$ compared to aniline. Currently, it is impossible to define unambiguously whether the reason for this increase is the elongation of the aromatic residue. Most probably, it lies in the exaggerated planarity invoked by AM1.

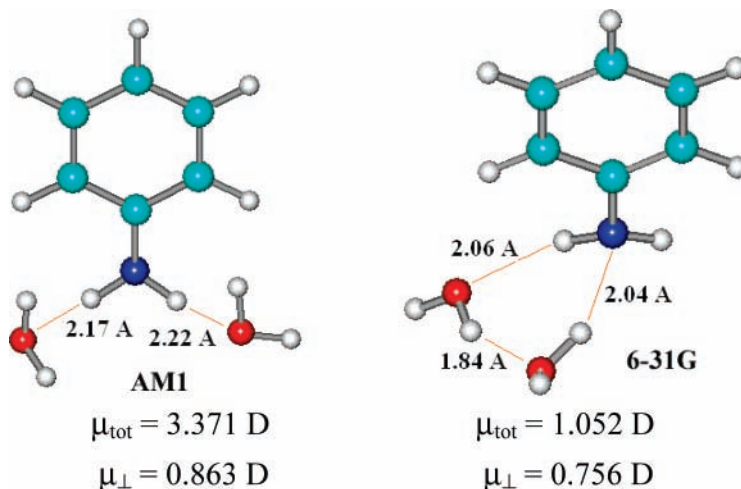


Figure 7. AM1 and RHF/6-31G optimized cluster of aniline with two water molecules.

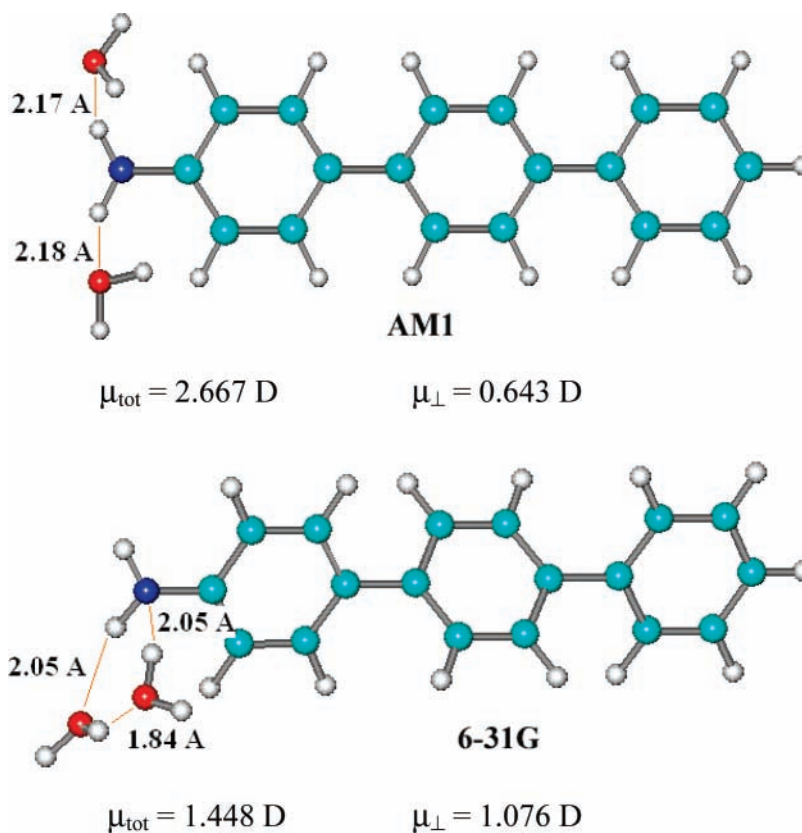


Figure 8. Optimized structure and calculated dipole moments of a cluster of 4-amino-*p*-terphenyl with two water molecules.

Quantitatively, both methods predict values for the normal component of the dipole moment, which are still too high compared to the estimate from the phenomenological model (see Table 1). This is an indication that the model may still be too simple.

To trace the influence of different polar parts of the surfactants on the structure and the electric properties of the monolayers, it is necessary to perform the calculations for molecules with the same hydrocarbon tail and various polar heads as done by Demchak and Fort in their original work.⁶ For the purpose, in addition to the amines, a series of clusters of aliphatic carboxylic acids, **12**–**16**, with two water molecules is optimized with RHF/6-31G. The starting topologies shown in Figure 9 are constructed (illustrated on the example of acetic acid). The geometry relaxation yielded three types of structures, as shown in Figure 10. The lowest energy geometries of **12**, **15**, and **16** correspond

to the one depicted in Figure 10b, in which one water molecule takes part in the formation of hydrogen bonds both with the carbonyl oxygen and with the hydroxyl hydrogen from the acid. The second water molecule is not directly coordinated by the acid but is rather hydrogen bonded to the first one. The energy difference in favor of structure **b** relative to **c** is ~ 3 – 4 kcal/mol (Table 3), regardless of the length of the hydrocarbon residue.

For the clusters of **13** and **14** the minimum energy structures are **c** and **a** from Figure 10, respectively. The common characteristic of all optimized structures is that three hydrogen bonds are formed with the carbonyl oxygen, and the acidic hydroxyl hydrogen is involved in two of them. Structure **b** has the advantage that one of the water molecules forms the maximum possible number of hydrogen bonds. The results for **15** and **16** are an indication that **b** will be the preferred structure

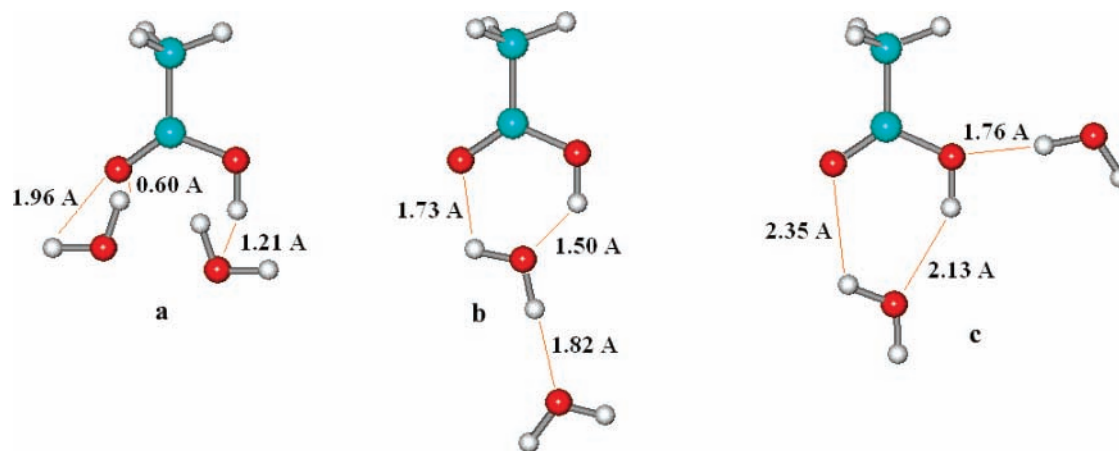


Figure 9. Scheme of the starting topology of a cluster built of acetic acid and two water molecules.

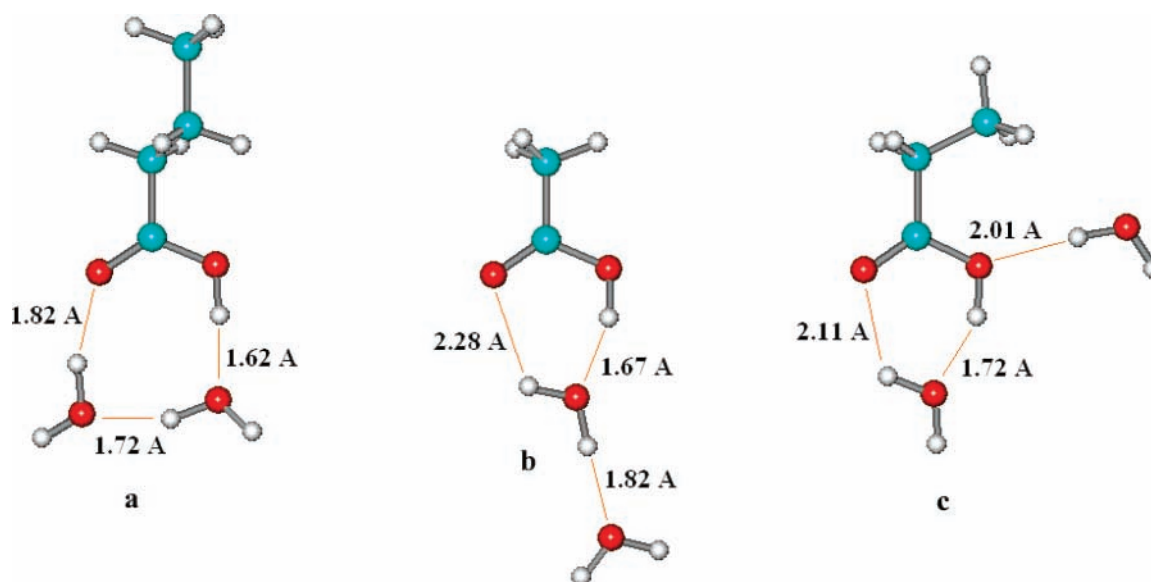


Figure 10. Optimized structures of clusters of aliphatic carboxylic acids with two water molecules.

TABLE 3: RHF/6-31G Calculated Total Energies of Clusters of Acids 12, 15 and 16 with Two Water Molecules with Coordination b and c (cf. Figure 10 for Structure Notation)

acid	type	energy, kcal/mol	$E(c) - E(b)$, kcal/mol
12	b	-238270.706	2.757
	c	-238267.949	
15	b	-311766.436	3.917
	c	-311762.519	
16	b	-336254.232	3.905
	c	-336250.327	

TABLE 4: RHF/6-31G Calculated Total (μ_{tot}) and Normal (μ_{\perp}) Dipole Moments of the Optimized Lowest Energy Clusters of Aliphatic Carboxylic Acids with Two Water Molecules

acid	μ_{tot} , D	μ_{\perp} , D
12b	4.778	4.687
13c	3.341	2.666
14a	0.567	0.538
15b	4.816	4.363
16b	4.854	4.297

for the long-chain aliphatic acids. Structures **a** and **c** are obviously intermediate for the three- and four-carbon atom acids, which have no dominance of the hydrophilic or of the hydrophobic part in their molecules.

The calculated dipole moments for the series of carboxylic acids 12–16 are collected in Table 4.

When preferred, structure **b** features the largest dipole moment, both total and normal. μ_{tot} increases relative to the isolated molecules by more than 2 D. This result is substantially different from the one obtained for the aliphatic amine **1** for which the total dipole moment does not change considerably upon addition of the two water molecules. The dissimilarity is due to the stabilization of different arrangements around the various polar heads. There is also a large diversity in the

magnitudes of the normal dipole moments of the amine and of the acids—for the latter μ_{\perp} is much larger, which is in line with the experimental results as well (0.360 D for tetradecanoic acid), although the calculated values are by an order of magnitude larger than the ones evaluated experimentally.²³

As the results presented so far reveal, the behavior of real monolayers at the air/water interface can be described quantitatively by calculating neither the structure (properties) of the isolated surfactant molecules nor those of small clusters containing one or two water molecules situated appropriately around the polar head of the organic molecule. Evidently, it is necessary to include a larger portion of the solvent surrounding, since it seems to be an important factor determining the properties of the monolayer. If the size of the clusters is increased, however, the use of the ab initio approach becomes

TABLE 5: Calculated Total (μ_{tot}) and normal (μ_{\perp}) AM1 Dipole Moments of Clusters of **5 Including Different Numbers of Water Molecules**

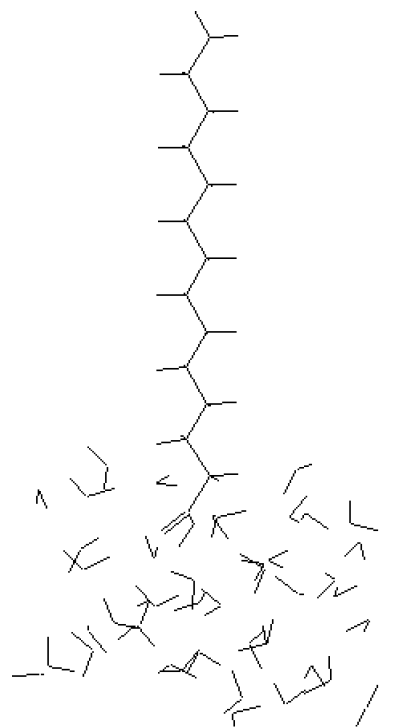
cluster	μ_{\perp} , D	μ_{tot} , D
5	2.067	2.384
5 + 2H ₂ O	0.643	2.667
5 + 6H ₂ O	2.966	4.217
5 + 11H ₂ O	2.158	4.849
5 + 20H ₂ O	4.686	4.728
two molecules of 5	4.587	4.587
2 molecules of 5 + 19H ₂ O	0.829 ^a	4.663 ^a

^a μ_{\perp} is recalculated for one molecule **5** with the water molecules belonging to it.

impractical due to the long computation times. Therefore, further calculations on larger clusters are performed at the semiempirical level.

3. Clusters with Inclusion of Larger Number of Water Molecules. 3.1. Models of *p*-Aminoterphenyl (5**).** The AM1 method is used for structure relaxation of clusters of **5** (built of one or two surfactant molecules) with different number of water molecules surrounding the polar head. The water environment is constructed by means of a periodic box with dimensions $15 \times 5 \times 30 \text{ \AA}$ (the first two dimensions are parallel to the film plane, and the third one is perpendicular to the water surface). The water molecules surrounding the hydrocarbon tails are removed, thus creating a “monolayer surface”. The water molecules in the periodic box are pre-equilibrated by a Monte Carlo simulation.²⁴ The values of the calculated dipole moments corresponding to the optimized structures are summarized in Table 5. The data show that the total dipole moment starts to increase and reaches some saturation for the last two clusters upon increase of the amount of water around the amino group of one molecule **5**. μ_{tot} of the two largest clusters is higher than that of an isolated molecule **5**, which is an indication that the water molecules from the surface contribute with some uncompensated dipole moment. This means that it is necessary to include at least 10 water molecules for correct description of all interactions at the monolayer surface. Unlike the total dipole moment, its normal component does not show any saturation upon increase of the amount of water. On the contrary, μ_{\perp} increases in a nonproportional manner and deviates more and more from the value estimated by Demchak and Fort for the corresponding monolayer (-0.095 D).⁶ As the total dipole moment does not vary after addition of more water, the solvent amount cannot be the reason for this discrepancy. Instead, it may be due to the fact that the lateral surfactant–surfactant interactions are not taken into account. This is confirmed by the results for the last cluster, constructed from two amines and 19 water molecules. Its total dipole moment practically does not change while μ_{\perp} decreases substantially and comes closer to the experimental value.⁶ It is noteworthy that the total dipole moment has a significant contribution from the water molecules although its value is very similar to μ of a cluster of two molecules **5** in vacuo. Upon addition of water, the latter decreases from 4.587 to 2.625 D, while the water dipole moment points in the opposite direction and amounts to 7.077 D.

3.2. Models of Carboxylic Acids (16** and **17**).** The same approach is applied to clusters of two carboxylic acids—hexanoic (C₅H₉COOH) acid (**16**) and tetradecanoic (C₁₃H₂₇COOH) acid (**17**)—since the latter forms monolayers, which are described experimentally and there are accessible data for the normal dipole moment, estimated with the Helmholtz model.²³ As for the clusters of **5**, the first step is to inspect the effect of increasing the amount of water on the dipole moment of a cluster



17

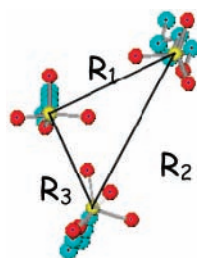
Figure 11. AM1 optimized structure of a myristic acid at the gas/water interface.

including one hydrated **17** (Figure 11). The calculated normal components of the dipole moment are shown in Table 6.

The calculated μ_{\perp} increases with the size of the aqueous environment and with 45 water molecules it reaches a steady value. This tendency is identical to the one witnessed for the amine **5**. Moreover, the magnitude of μ_{\perp} is overestimated appreciably too.

The effect of intermolecular interactions is studied on clusters of **16**. The simulated clusters contain up to five acid molecules with polar heads surrounded by different number of water molecules. The AM1 optimized structures are illustrated in Figure 12.

Different starting geometries of the clusters are tested, linear alignment of the acid molecules in this number. In cases **c–e**, however, the optimization always converges to grouping indicative of the tendency of domain formation. This can be attributed to tighter packing of both the heads and the tails of the hydrated acids, evidenced by the estimates of area per solvated molecule (**A**) calculated in spherical approximation according to the relation: $A = \pi(1/N \sum_{i=1}^N R_i/2)^2$; N = number of surfactant molecules in the cluster as illustrated by the example of three molecules presented in the following scheme:



$$A = \pi \left(\frac{1}{3} \sum_{i=1}^3 \frac{R_i}{2} \right)^2$$

It should be noted that this strategy yields an “effective” area per molecule, i.e., it accounts for the adhering water. Thus, we

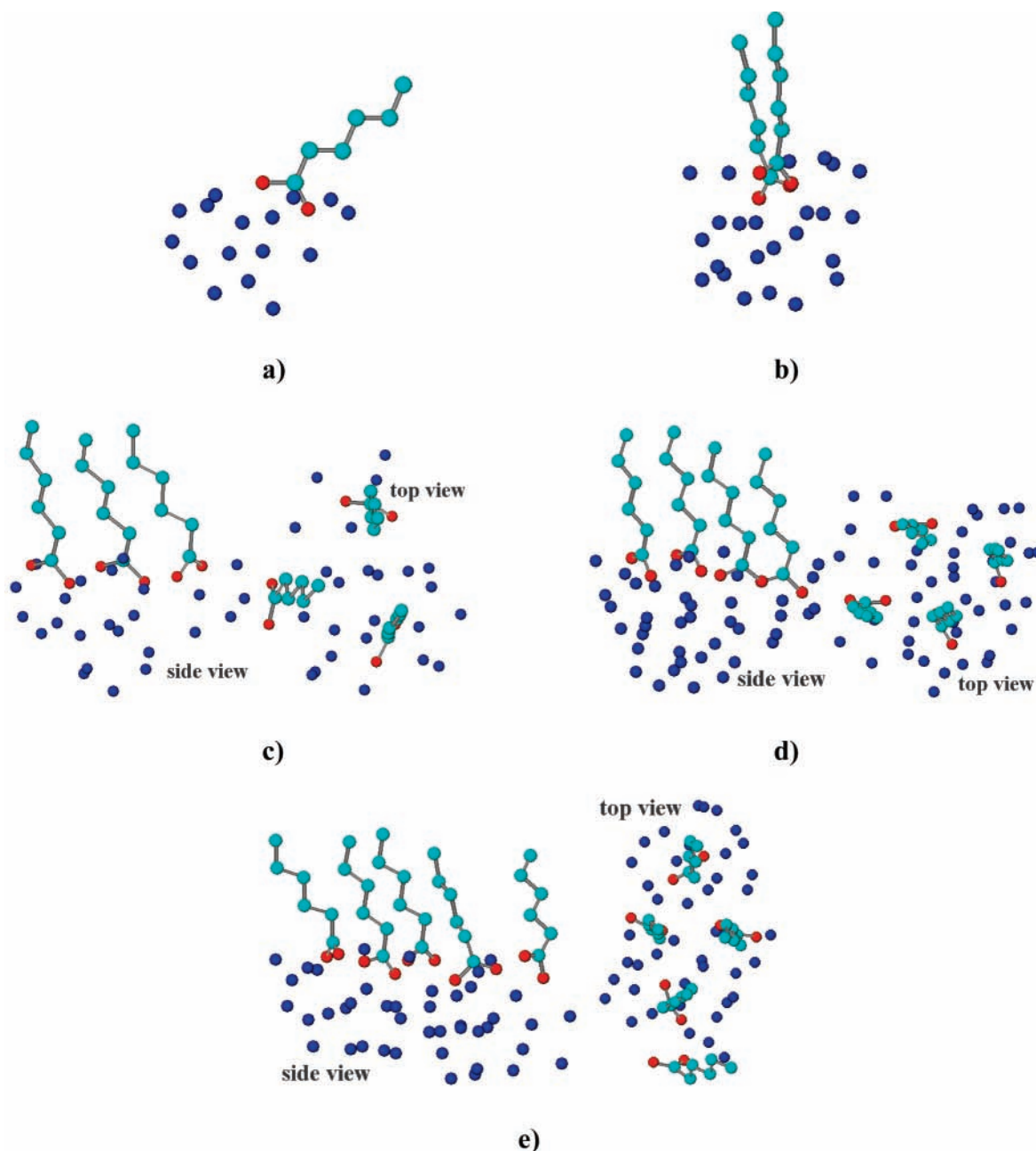


Figure 12. Schemes of AM1 optimized geometry of clusters containing different number (1–5—cases a–e) of adequately hydrated amphiphilic molecules **16** at the gas/water interface. The hydrogen atoms are omitted for clarity.

TABLE 6: Calculated normal (μ_{\perp}) AM1 Dipole Moments of Clusters of **17** Including Different Numbers of Water Molecules

no. of H ₂ O	μ_{\perp} , D
25	0.947
35	1.188
45	1.873
55	1.889

mimic the conditions of the experimental estimations we are testing our models against. The calculated areas per molecule and dipole moment contributions of all investigated clusters of **16** are collected in Table 7.

The increase of cluster size (amount of surfactant and water molecules) causes a decrease of the average distance between carboxyl groups and the area per molecule due to enhanced attraction among a greater number of neighbors in the nano-domain. The results for **A** obtained theoretically compare nicely to the experimentally found values (20.4 Å²) for compressed

TABLE 7: Calculated Average Intersurfactant Distances (R), Effective Area per Molecule (A), and Total (μ_{tot}) and Normal (μ_{\perp}) Dipole Moment per Surfactant Molecule of AM1 Optimized Clusters of Hydrated Hexanoic Acid^a

no. of amphiphilic molecules	no. of water molecules	R , Å	A , Å ²	μ_{tot} , D	μ_{\perp} , D
1	16			2.061	1.836
2	24	5.20	21.3	2.139	0.628
3	24	5.07	20.2	2.405	1.981
4	41	4.95	19.2	1.173	0.930
5	44	4.74	17.7	1.518	1.391

^a The values for R and A are taken from an earlier paper.²⁵

monolayer of myristic acid.²³ The slightly lower computed values reflect the lack of thermal motion in the theoretical model.

The total dipole moment and its normal component oscillate, being lower for even and higher for odd number of acid molecules in the cluster, which can be attributed to the higher

ordering (tighter packing) of the former and lower of the latter systems. Nevertheless, the values converge with cluster growth to a value, lower than those of the single hydrated acid molecules. This is due to two synergetic factors: water organization around the polar head compensating partly for the intrinsic dipole moment of the acid and dipole–dipole interaction of surfactant molecules (markedly expressed in the cluster of two acidic molecules).

The latter models include most of the factors, essential for the behavior of amphiphilic molecules at the gas/water interface—adequate aqueous environment and intermolecular interaction with more than one neighboring surfactant. The structural parameters reflect properly the experimental data, but the calculated values of the normal component of the dipole moment are still higher than the ones estimated from the phenomenological models. Most probably, the reason for this mismatch is the effective dielectric constant assigned to each part of the dipole in the three-capacitor model. The quantum-chemical simulations account for the dielectric properties of the monolayer in an explicit manner—through the specific intermolecular interactions between the dipoles. This difference in the two approaches prohibits quantitative agreement between the values of μ_{\perp} obtained within our models and those reported on the basis of the phenomenological schemes. Furthermore, we believe that complete match of the numeric values is evasive. The above computational results indicate that depending on the type of the polar headgroup, the structure of the surrounding water is different, which is reflected directly by the calculated dipole moments. Thus, we consider the proposed models as promising with respect to the possibility for estimation of an effective dielectric constant specific for each monolayer, without the need of artificial partitioning of the system. We have proposed a simple way to obtain such values for the dielectric constant²⁶ based on the Helmholtz equation, provided that there are data for the surface potential of the monolayer. Another advantage of the proposed models is that they take into account explicitly the organization of water molecules around the surfactant heads and its contribution to the dipole moment, which may be significant but is often neglected in the capacitor models.

Conclusions

Quantum chemical calculations at different levels of theory are performed for a number of organic molecules—short-tail analogues of surfactants forming insoluble monolayers at the air/water interface. The influence of the nearest neighboring water molecules on the structure and the dipole moment of the organic molecules is studied. For this purpose, model clusters containing different number of water molecules are optimized.

Optimization of the organic molecules in vacuo with different theoretical methods reveals that RHF/6-31G and AM1 reproduce most correctly the experimental dipole moments of the isolated molecules. The values, however, are much higher than the ones measured for monolayers at the water surface. Thus, inclusion of the water surrounding is indispensable.

The results from the ab initio calculations on clusters of three different amines show that the arrangement of the water molecules around the polar amino group is not affected materially by the nature of the hydrocarbon tail, i.e., aliphatic or aromatic, which is in accord with findings from the phenomenological models.^{11c} In all cases, the maximum number of hydrogen bonds is sought, both between water and amine and between water molecules themselves. There is no major difference in the calculated total dipole moments of aromatic and aliphatic clusters as well, but the normal components are

not alike and vary more markedly with the particular system. For the clusters studied, μ_{\perp} is in the range 0.374–1.070 D.

The results for clusters with the same tails but different polar heads indicate that the electric properties of the clusters are highly sensitive to the nature of the polar head and that each surfactant type has to be treated specifically. The dependence of the dipole moment on the hydrophobic tail length is much less pronounced. The values of μ (for the same type of structure) practically do not change for tail length beyond four carbon atoms, which coincides with the estimates of Taylor and Bayes.⁸

All factors considered, quantum chemically computed dipole moments will always differ from the phenomenologically estimated ones as the latter with no exception borrow *constant* dielectric parameters for seemingly similar and yet different compounds with no account for the interface anisotropy and the dependence of the parameters on the organization of surfactant and water molecules.

These results indicate that the parameters used in the phenomenological models for interpretation of surface potential data of monolayers have to be adopted with care when dealing with monolayers composed of substantially different surfactants.

In summary, the theoretical simulation of small clusters of organic molecules with their closest aqueous surrounding provides part of the desired microscopic information on the parameters governing the surfactant behavior within insoluble monolayers of organic surfactants. It is seen that the arrangement around the polar heads is mostly hydrogen bonding controlled. Consequently, the effective dipole moment of the molecules at the interface is determined by the local structural arrangement of the polar head but there is also a significant contribution from the surface water molecules. For correct estimates of the monolayer dipole moments, the lateral interaction between neighboring surfactants has to be taken into account as well.

Acknowledgment. The work was supported by Project X-1305 of the National Scientific Research Fund at the Bulgarian Ministry of Education and Science.

References and Notes

- (1) Davies, J.; Rideal, E. *Interfacial Phenomena*; Academic Press: New York, 1961. Gaines, G. *Insoluble Monolayers at Liquid–Gas Interfaces*, Wiley-Interscience, New York, 1966.
- (2) Adamson, W. *Physical Chemistry of Surfaces*, 5th ed.; Wiley-Interscience: New York, 1990; p 113.
- (3) Moehwald, H. *Annu. Rev. Phys. Chem.* **1990**, *41*, 441–476.
- (4) Hoening, D.; Moebius, D. *J. Phys. Chem.* **1991**, *95*, 4590–4592.
- (5) Lee, L.; Mann, E.; Langevin, D.; Farnoux, B. *Langmuir* **1991**, *7*, 3076–3081.
- (6) Demchak, R.; Fort, T. *J. Colloid Interface Sci.* **1974**, *46*, 191.
- (7) Vogel, V.; Moebius, D. *Thin Solid Films* **1988**, *159*, 73.
- (8) Taylor, D.; Bayes, G. *Phys. Rev. E* **1994**, *49*, 1439.
- (9) Ivanova, Tz.; Grozev, N.; Panaiotov, I.; Proust, J. *Colloid Polym. Sci.* **1999**, *277*, 709.
- (10) Brasseur, R. In *Molecular Description of Biological Membrane Components by Computer-Aided Conformational Analysis*; Brasseur, R., Ed.; CRC: Boca Raton, FL, 1990; Vol. 1, p 203.
- (11) (a) Petrov, J.; Polymeropoulos, E.; Moehwald, H. *J. Phys. Chem.* **1996**, *100*, 9860. (b) Dynarowicz-Latka, P.; Cavalli, A.; Silva Filho, D. A.; dos Santos, M. C.; Oliveira, O. N. *Chem. Phys. Lett.* **2000**, *326*, 39. (c) Dynarowicz-Latka, P.; Cavalli, A.; Silva, D. A.; Milart, P.; dos Santos, M. C.; Oliveira, O. N. *Chem. Phys. Lett.* **2001**, *337*, 11.
- (12) Wilson, M.; Pohorille, A. *J. Am. Chem. Soc.* **1994**, *116*, 1490.
- (13) Hoshi, H.; Sakurai, M.; Inoue, Y.; Chujo, R. *J. Mol. Struct. (THEOCHEM)* **1988**, *180*, 267.
- (14) Johann, R.; Brezesinski, G.; Vollhardt, D.; Moehwald, H. *J. Phys. Chem. B* **2001**, *105*, 2957.
- (15) Miranda, P. B.; Du, Q.; Shen, Y. R. *Chem. Phys. Lett.* **1998**, *286*, 1.
- (16) Avila, L.; Saraiva, S.; Oliveira, J. *Colloids Surf.* **1999**, *154*, 209.
- (17) Allinger, N. *J. Am. Chem. Soc.* **1977**, *99*, 8127. Allinger, N.; Yuh, Y. Quantum Chemistry Program Exchange, Bloomington, IN, Program

#395. Burkert, U.; Allinger, N. *Molecular Mechanics*; ACS Monograph 177; American Chemical Society; 1982.

(18) Dewar, M.; Zoebisch, E.; Healy, E.; Stewart, J. *J. Am. Chem. Soc.* **1985**, *107*, 3902.

(19) Frisch, M. J.; Trucks, G. W.; Schlegel, H. B.; Scuseria, G. E.; Robb, M. A.; Cheeseman, J. R.; Montgomery, J. A., Jr.; Vreven, T.; Kudin, K. N.; Burant, J. C.; Millam, J. M.; Iyengar, S. S.; Tomasi, J.; Barone, V.; Mennucci, B.; Cossi, M.; Scalmani, G.; Rega, N.; Petersson, G. A.; Nakatsuji, H.; Hada, M.; Ehara, M.; Toyota, K.; Fukuda, R.; Hasegawa, J.; Ishida, M.; Nakajima, T.; Honda, Y.; Kitao, O.; Nakai, H.; Klene, M.; Li, X.; Knox, J. E.; Hratchian, H. P.; Cross, J. B.; Adamo, C.; Jaramillo, J.; Gomperts, R.; Stratmann, R. E.; Yazyev, O.; Austin, A. J.; Cammi, R.; Pomelli, C.; Ochterski, J. W.; Ayala, P. Y.; Morokuma, K.; Voth, G. A.; Salvador, P.; Dannenberg, J. J.; Zakrzewski, V. G.; Dapprich, S.; Daniels, A. D.; Strain, M. C.; Farkas, O.; Malick, D. K.; Rabuck, A. D.; Raghavachari, K.; Foresman, J. B.; Ortiz, J. V.; Cui, Q.; Baboul, A. G.; Clifford, S.; Cioslowski, J.; Stefanov, B. B.; Liu, G.; Liashenko, A.; Piskorz,

P.; Komaromi, I.; Martin, R. L.; Fox, D. J.; Keith, T.; Al-Laham, M. A.; Peng, C. Y.; Nanayakkara, A.; Challacombe, M.; Gill, P. M. W.; Johnson, B.; Chen, W.; Wong, M. W.; Gonzalez, C.; Pople, J. A. *Gaussian 03*, revision B.04. Gaussian, Inc.: Pittsburgh, PA, 2003.

(20) *HYPERCHEM 7.03*. Hypercube Inc.: Gainsville, FL.

(21) Minkin, V.; Osipov, O.; Gdanov, U. In *Dipole moments in Organic Chemistry*; Khimia: Leningrad, USSR, 1968 (in Russian).

(22) Dynarowicz-Łatka, P. D.; Kita, K. *Adv. Colloid Interface Sci.* **1999**, *79*, 1.

(23) Panayotov, I. *Introduction to Biophysical Chemistry*; Nauka i izkustvo: Sofia, 1982 (in Bulgarian).

(24) Metropolis, N.; Rosenbluth, A. W.; Rosenbluth, M. N.; Teller, A. H.; Teller, E. *J. Chem. Phys.* **1953**, *21*, 1087.

(25) Ivanova, A.; Tadjer, A.; Radoev, B.; Panayotov, I. *SAR QSAR Environm. Res.* **2002**, *13*, 237.

(26) Ivanova, A.; Tadjer, A.; Radoev, B. *Int. J. Quantum Chem.* **2002**, *89*, 397.